Quantum spin Hall effect in a square-lattice model under a uniform magnetic field*

Guo Huai-Ming(郭怀明)[a)†] and Feng Shi-Ping(冯世平)[b)]

[a)] *Department of Physics, Beihang University, Beijing* 100191, *China*

[b)] *Department of Physics, Beijing Normal University, Beijing* 100875, *China*

(Received 3 January 2012; revised manuscript received 7 February 2012)

We study a toy square-lattice model under a uniform magnetic field. Using the Landauer–Büttiker formula, we calculate the transport properties of the system on a two-terminal, a four-terminal and a six-terminal device. We find that the quantum spin Hall (QSH) effect appears in energy ranges where the spin-up and spin-down subsystems have different filling factors. We also study the robustness of the resulting QSH effect and find that it is robust when the Fermi levels of both spin subsystems are far away from the energy plateaus but is fragile when the Fermi level of any spin subsystem is near the energy plateaus. These results provide an example of the QSH effect with a physical origin other than time-reversal (TR) preserving spin-orbit coupling (SOC).

Keywords: quantum spin Hall effect, topological insulator

PACS: 73.43.–f, 72.25.Hg, 73.20.–r, 85.75.–d **DOI:** 10.1088/1674-1056/21/7/077303

1. Introduction

Recently, a new class of topological quantum states have emerged in condensed matter physics, called topological insulators (TIs).[1−7] They differ from ordinary insulators in that they have a topologically protected edge or surface states traversing the gap. Moreover, these edge or surface states are protected by time-reversal (TR) symmetry and are very robust to non-magnetic disorders. This makes TIs exhibit many unusual physical properties and show potential applications in spintronics and fault tolerant quantum information processing.[8−11]

The study of TIs grew out of the work on the quantum spin Hall (QSH) effect in non-magnetic materials with spin-orbit coupling (SOC).[12,13] In the late 1980s it was found that the quantum Hall effect can be also driven by a SOC in the absence of a uniform magnetic field.[14] SOC is a spin-dependent force originated from a relativistic effect most common in heavy elements. Since it preserves TR symmetry, it can lead to the QSH effect in electron systems with vanishing Hall conductance. Later, it is realized that the resulting QSH state is a new quantum state, TI, which is described by a new type of Z_2- valued topological invariant.[15]

In TR invariant two-dimensional (2D) TIs, the helical edge state is the key characteristic and it naturally gives rise to the QSH effect. Thus, 2D TIs are also synonymously referred to as QSH insulators. However, the QSH effect does not necessarily exist in 2D systems with TR preserving SOC. Instead, it can also be induced by other physical origins, which may break TR symmetry.[16,17] One such example is the study on the QSH effect in ferromagnetic graphene.[17] Though the predicted QSH effect is still caused by the edge states, the two states on each edge are related by charge conjugation–TR combined (instead of TR) transformation. Motivated by this idea, in this paper, we construct a square-lattice model under a uniform magnetic field and realize the QSH effect in the absence of TR preserving SOC.

2. The model and method

We consider a square lattice model with a tight-binding Hamiltonian[18,19]

$$H = -\sum_{\langle ij\rangle\sigma} t_{ij}\,\mathrm{e}^{\mathrm{i}\theta_{ij}} c^{\dagger}_{j\sigma} c_{i\sigma} + \sum_{i,\sigma} \sigma M c^{\dagger}_{i\sigma} c_{i\sigma}, \qquad (1)$$

where $c^{\dagger}_{i\sigma}$ and $c_{i\sigma}$ are the annihilation and creation operators at site $\boldsymbol{r}_i$. Here, t_{ij} are hopping amplitudes between nearest-neighbor sites with $t_{i,i+\hat{x}} = t$

*Project supported by the National Natural Science Foundation of China (Grant Nos. 11104189 and 11074023) and the National Basic Research Program of China (Grant Nos. 2011CBA00102, 2011CB921700, and 2012CB821403).

†Corresponding author. E-mail: hmguo@buaa.edu.cn

© 2012 Chinese Physical Society and IOP Publishing Ltd

and $t_{i,i+\hat{y}} = (-1)^{x_i} t$, as shown in Fig. 1(a). The magnetic field is included through Peierls phase factors, $\theta_{ij} = (2\pi/\Phi_0) \int_{\boldsymbol{r}_i}^{\boldsymbol{r}_j} \boldsymbol{A} \cdot \mathrm{d}\boldsymbol{l}$ with $\boldsymbol{A}$ the vector potential and $\Phi_0 = hc/e$ the magnetic flux quantum. We chose the Landau gauge $\boldsymbol{A} = (-By, 0)$ where we set the lattice constant unity. M is the ferromagnetic exchange split which acts on different spins with different signs ($\sigma = 1$ for up-spin and $\sigma = -1$ for down-spin).

In the absence of a magnetic field, the system has translational symmetry. We may choose a two-site unit cell $(i, i + \hat{x})$ and form a spinor field $\psi_{i\sigma} = (c_{i\sigma}, c_{i+\hat{x}\sigma})^{\mathrm{T}}$. The Hamiltonian can be written compactly in the reciprocal space as

$$H = \sum_{\boldsymbol{k},\sigma} \psi^{\dagger}_{\boldsymbol{k}\sigma} \mathcal{H}_{\boldsymbol{k}\sigma} \psi_{\boldsymbol{k}\sigma} \tag{2}$$

in the reduced Brillouin zone $\{\boldsymbol{k} : 0 \leq k_x < \pi, 0 \leq k_y < 2\pi\}$ with $\mathcal{H}_{\boldsymbol{k}\sigma} = \sigma M - 2t[\cos(k_x)\sigma_x + \cos(k_y)\sigma_z]$, where σ_x and σ_z are Pauli matrices. The energy spectrum of $\mathcal{H}_{\boldsymbol{k}\sigma}$ is given by

$$E_{\boldsymbol{k}\sigma} = \sigma M \pm \sqrt{\cos^2 k_x + \cos^2 k_y}. \tag{3}$$

For $M = 0$, as shown in Fig. 1(b), the energy spectrum is symmetric around zero and has two inequivalent Dirac points $\boldsymbol{K}_{1,2} = (\pi/2, \pi/2), (\pi/2, 3\pi/2)$. When the system is subjected to a perpendicular magnetic field, the energy bands evolve into the Landau levels, which are shown in Figs. 1(c) and 1(d). The ferromagnetic term shifts the energy bands of spin-up and spin-down subsystems oppositely, generating ranges with different filling factors for different spins. We will show by explicit numerical calculations in what follows that the QSH effect exists in these ranges.

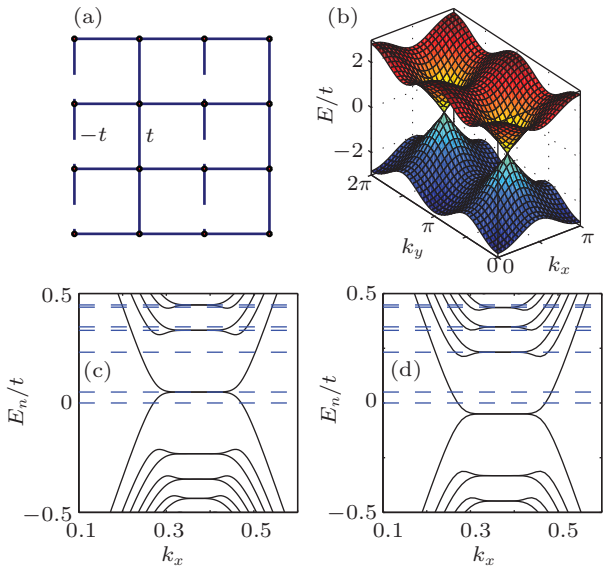


Fig. 1. (colour online) (a) The square lattice on which our model resides(the solid and dashed lines represent the signs of the hopping amplitudes between the nearest-neighbor sites). (b) The spectrum of the lattice model for $M = 0$ and without a magnetic field. (c) and (d) are the energy spectrum of a strip of width $N_y = 80$ sites with open boundary conditions along y and infinite along x for $M = 0.05$ and under a uniform magnetic field with a flux of $\phi = 0.01\Phi_0$ threading each plaquette, where (c) and (d) are for spin-up and spin-down subsystems respectively. The blue dashed lines in (c) and (d) are the guidelines of the positions of the Landau levels.

We use the Landauer–Büttiker formula to study the QSH effect of the system,[20−22] where the current flowing through the leads can be formulated as

$$I_{p\sigma} = -\frac{e}{h} \sum_{q} \int \mathrm{d}E T_{pq\sigma}(E)[f_p(E) - f_q(E)], \tag{4}$$

where p, q label the different leads, $f_p(E) = 1/\{\exp[(E - eV_p)/k_{\mathrm{B}}T] + 1\}$ is the Fermi–Dirac distribution for lead p. The transmission coefficient $T_{pq\sigma}(E)$ from the leads q to p with spin σ can be calculated from the equation $T_{pq\sigma}(E) = \mathrm{Tr}[\boldsymbol{\Gamma}_{p\sigma} \boldsymbol{G}^{\mathrm{r}}_{\sigma} \boldsymbol{\Gamma}_{q\sigma} \boldsymbol{G}^{\mathrm{a}}_{\sigma}]$ with the linewidth function $\boldsymbol{\Gamma}_{p\sigma}(E) = \mathrm{i}[\boldsymbol{\Sigma}^{\mathrm{r}}_{p}(E) - \boldsymbol{\Sigma}^{\mathrm{a}}_{p}(E)]$, the Green functions $\boldsymbol{G}^{\mathrm{r}}_{\sigma}(E) = [\boldsymbol{G}^{\mathrm{a}}_{\sigma}(E)]^{\dagger} = 1/(E - \boldsymbol{H}^{\mathrm{cen}}_{\sigma} - \sum_p \boldsymbol{\Sigma}^{\mathrm{r}}_{p\sigma})$ and the Hamiltonian in the center region $\boldsymbol{H}^{\mathrm{cen}}_{\sigma}$, the retarded self-energy $\boldsymbol{\Sigma}^{\mathrm{r}}_{p\sigma}(E)$. For small voltages between the leads and zero temperature, the Landauer–Büttiker formula can be simplified as

$$I_{p\sigma} = \frac{e^2}{h} \sum_{q} T_{pq\sigma}(E_{\mathrm{F}})[V_p - V_q], \tag{5}$$

where E_{F} is the Fermi energy of the system. Thus, the conductances and resistances of the devices can be fully determined by calculating the transmission coefficients between the leads.

3. Numerical results for clean systems

We consider a two-terminal, a four-terminal, and a six-terminal device under a high magnetic field and carry out explicit calculations to study the QSH effect on the system. In the following calculations, we fix the flux threading each plaquette to be $\phi = 0.01\Phi_0$ and the system size to be $N = 80$ sites (the widths of the leads and the length of the central region).

3.1. The two-terminal device

We first consider the two-terminal device (see the inset of Fig. 2). A small bias V is applied between leads 1 and 2. The calculated conductance is shown in Fig. 2. For both cases ($M = 0$ and $M = 0.05$), the

conductance shows quantized plateaus. Since at zero temperature only the carriers at the Fermi energy contribute to the conductance, the quantized values equal half the number of the crossings (in unit of $2e^2/h$) between the Fermi energy and the bands. The numerical results are consistent with the above argument.

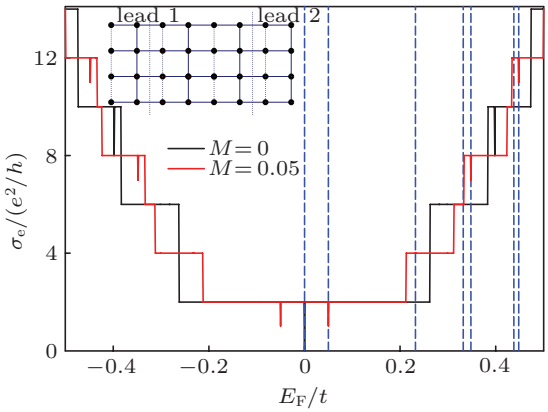


Fig. 2. (colour online) The longitudinal conductance σ_e versus the Fermi energy E_F. The blue dashed lines correspond to those in Figs. 1(c) and 1(d). The two-terminal device is schematically shown in the inset.

For systems subjected to a perpendicular magnetic field, the energy bands evolve into Landau levels and the electrons are distributed near the edges of the system. In Fig. 3, we show the density distributions at four different energies. It shows that the conducting electron becomes more localized near the edge as the energy level becomes farther away from the plateau in the energy bands. These plateaus are interesting places. As we increase the momentum along the plateau, the corresponding eigenvalue does not change. However, through the plateau the electron changes the edge on which it is localized. The edge states flow along the edges in the chirality determined by the magnetic field and the type of the carriers. Specifically, in our case, the edge state is clockwise (counter clockwise) for electron- (hole-) type carriers, which is schematically shown in Fig. 4 via the current distribution. For the case of $M = 0$, the subsystems of spin-up and spin -down electrons are identical and the whole system shows a quantum Hall effect. For the case of $M \neq 0$, there appear ranges $(-M < E_F/t < M)$ where the two subsystems have different chirality. As has been known, this will induce the QSH effect.

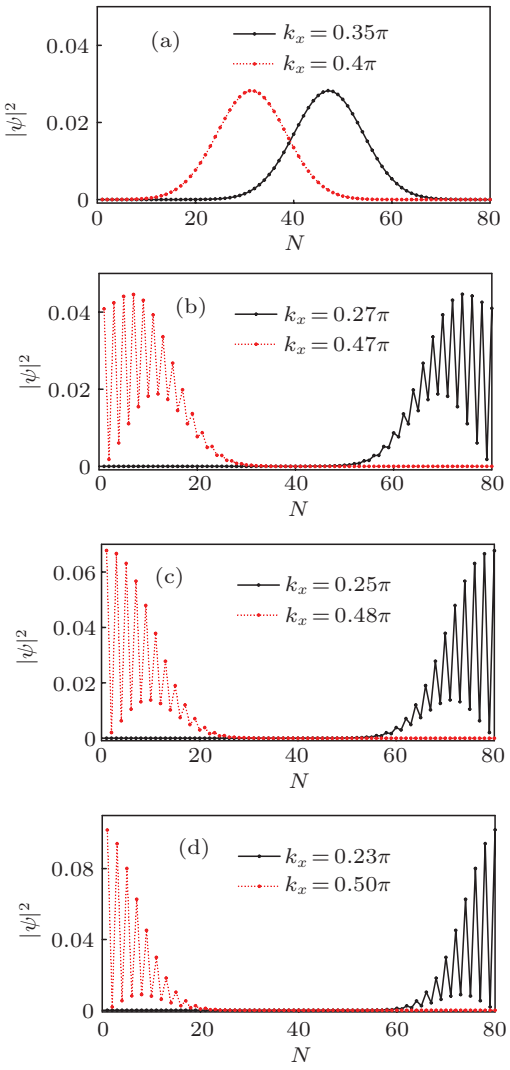


Fig. 3. (colour online) The density distributions of the edge states on a strip for $M = 0$, when the spin-up and spin-down subsystems are identical. The density distributions at the two momenta corresponding to the same energy: (a) the energy $E/t = 0$; (b) the energy $E/t = 0.05$; (c) the energy $E/t = 0.1$; (d) the energy $E/t = 0.2$.

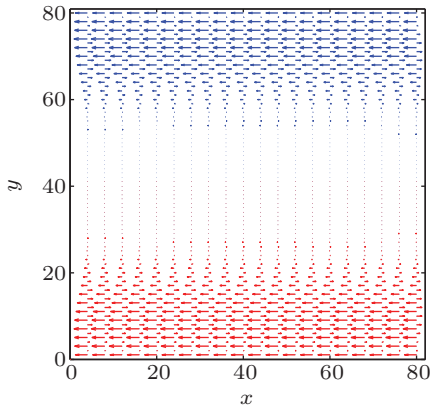


Fig. 4. (colour online) The current distribution of the edge states on a strip for $M = 0.05$ and $E_F/t = 0$. The carriers are holes for spin-up subsystem (blue arrows, the upper part) and electrons for spin-down subsystem (red arrows, the lower part).

3.2. The four-terminal device

We then consider the four-terminal device (see the inset of Fig. 5). A small bias V is applied between the longitudinal terminals 1 and 3. The transverse terminals 2 and 4 are used to probe the induced charge current $I_{\rm ne} = (I_{\rm n\uparrow} + I_{\rm n\downarrow})$ and spin current $I_{\rm ns} = (\hbar/2e)(I_{\rm n\uparrow} - I_{\rm n\downarrow})$. The voltages on the four terminals are $V_{1\sigma} = V/2$, $V_{3\sigma} = -V/2$, and $V_{2\sigma} = V_{4\sigma} = 0$. Since the currents in terminals 2 and 4 just differ in a sign, below we only show the currents in terminal 2. Figure 5 shows the results of the Hall conductance $\sigma_{\rm e}^{\rm H} = I_{\rm e}/V$ and the spin Hall conductance $\sigma_{\rm s}^{\rm H} = I_{\rm s}/V$ versus the Fermi energy $E_{\rm F}$. For the case of $M = 0$, $\sigma_{\rm s}$ is zero and $\sigma_{\rm e}$ exhibits quantized values at odd integer values ne^2/h ($n = \pm1, \pm3, \ldots$). A similar result has been experimentally observed in graphene where the electron transport is essentially governed by Dirac's equation.[23–26] The low-energy behavior of our toy model is also described by Dirac's equation, so naturally it shows a similar behavior to that in graphene. Using the Landauer–Büttiker formula Eq. (5), the Hall and spin Hall conductance can be analytically obtained to be $\sigma_{\rm e}^{\rm H} = (\nu_\uparrow + \nu_\downarrow)e^2/2h$ and $\sigma_{\rm s}^{\rm H} = (\nu_\uparrow - \nu_\downarrow)e/8\pi$ with ν_σ the Landau filling factor for spin σ. Since $\nu_\uparrow = \nu_\downarrow$ for $M = 0$ and ν_σ is always an odd integer, the Hall conductance gets odd integer values (in unit of e^2/h). From the above analytical formulas, we can see that $\sigma_{\rm s}$ gets a non-zero value when $\nu_\uparrow \neq \nu_\downarrow$. Therefore, the ferromagnetic exchange split term is included in Hamiltonian Eq. (1) to generate the differences of $\nu_\uparrow$ and $\nu_\downarrow$, realizing the QSH effect in the system. As shown in Fig. 5, for $M \neq 0$, a spin current emerges in the ranges with $\nu_\uparrow \neq \nu_\downarrow$ and the spin Hall conductance shows quantized plateaus. The quantized values from the numerical calculations are in good agreement with those obtained from the analytical formulas.

3.3. The six-terminal device

We next consider the six-terminal device (see the inset of Fig. 6). A small bias V is applied between the longitudinal terminals 1 and 4 ($V_{1\sigma} = V/2$, $V_{4\sigma} = -V/2$). The transverse terminals 2, 3, 5 and 6 are used to probe the voltages and the voltage values can be derived using the Landauer–Büttiker formula under the condition that their charge currents vanish. Then the longitudinal resistance $R_{14,23} = (V_2 - V_3)/I_{1\rm e}$ and Hall resistance $R_{14,26} = (V_2 - V_6)/I_{1\rm e}$ can be obtained. Their values can be analytically derived (in unit of h/e^2): for $(\nu_\uparrow, \nu_\downarrow)(>0, >0)$ or $(<0, <0)$, $R_{14,23} = 0$ and $R_{14,26} = (-1)/(\nu_\uparrow + \nu_\downarrow)$; $(\nu_\uparrow, \nu_\downarrow)(>0, <0)$ or $(<0, >0)$, $R_{14,23} = |\nu_\uparrow\nu_\downarrow|/(|\nu_\uparrow|^3 + |\nu_\downarrow|^3)$ and $R_{14,26} = {\rm sgn}(\nu_\uparrow)(|\nu_\downarrow|^2 - |\nu_\uparrow|^2)/(|\nu_\uparrow|^3 + |\nu_\downarrow|^3)$. The numerical results in Fig. 6 are in good agreement with the above analytical formulas, except in the regions where the Fermi levels are near the Landau levels. The

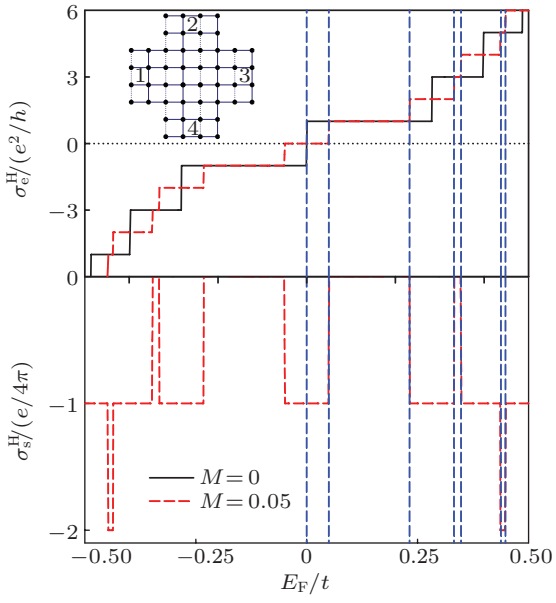


Fig. 5. (colour online) The Hall conductance $\sigma_{\rm e}^{\rm H}$ and spin Hall conductance $\sigma_{\rm s}^{\rm H}$ versus the Fermi energy $E_{\rm F}$. The blue dashed lines correspond to those in Figs. 1(c) and 1(d). The four-terminal device is schematically shown in the inset of the top panel.

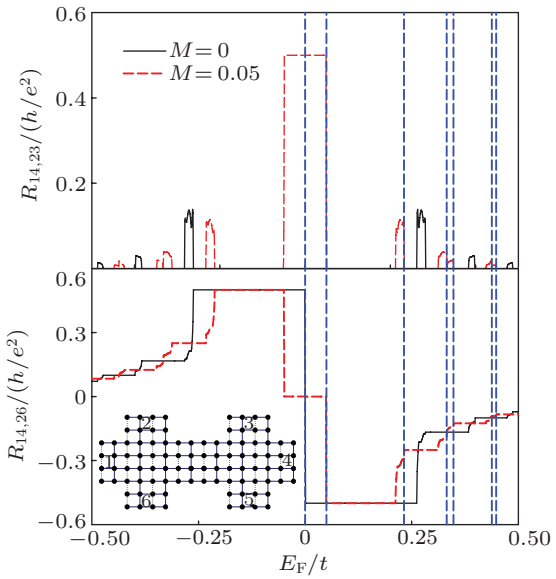


Fig. 6. (colour online) The longitudinal resistance $R_{14,23}$ and the Hall resistance $R_{14,26}$ versus the Fermi energy $E_{\rm F}$. The blue dashed lines correspond to those in Figs. 1(c) and 1(d). The six-terminal device is schematically shown in the inset of the bottom panel.

deviations are due to the dips near the Landau levels, which also contribute to the longitudinal current. However, in the analytical deriving, we do not include their contributions.

4. Robustness to disorder

Untill now, we have shown the existence of the QSH effect in the square-lattice model described by Eq. (1) through explicit numerical calculations and analytical deriving. The resulting QSH effect breaks TR symmetry and is different from the Z_2 QSH insulator, which comes from SOC and preserves TR symmetry. Since it has been well known that the Z_2 QSH insulator is very robust to non-magnetic disorder, naturally we ask how that disorder affects the stability of the present QSH effect. In what follows we study the robustness of the spin Hall conductance to disorder on the four-terminal device. To simulate the effects of disorder, we add a term $\sum_{j\sigma} U_j \psi^{\dagger}_{j\sigma}\psi_{j\sigma}$ to Hamiltonian Eq. (1), where U_j is a random on-site potential uniformly distributed in the range $(-U_0/2, U_0/2)$ with the disorder strength U_0. In the following calculations, we assume the disorder only exists in the central region and always keep the Fermi levels of the leads identical to that of the central region. For each disorder strength, the results are averaged over 500 independent disorder realizations. We carry out calculations at disorder strengths $U_0/t = 1, 2, 3$ and the results are shown in Fig. 7. It shows that the spin Hall conductance $\sigma_{\rm s}^{\rm H}$ is robust to the disorder. For small disorder strengths, the quantum plateau maintains its quantized value very well. With increasing disorder strengths, the spin Hall conductance only slightly decreases from the quantized value. In addition, even for a very large disorder strength such as $U_0/t = 3$, which can be compared with the band width, the spin Hall conductance still maintains a sizeable value.

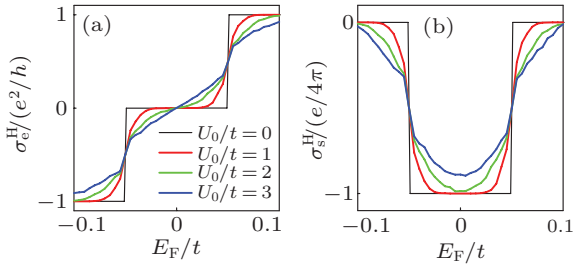


Fig. 7. (colour online) The robustness of the (a) Hall conductance $\sigma_{\rm e}^{\rm H}$ and (b) spin Hall conductance $\sigma_{\rm s}^{\rm H}$ to a disorder for $M = 0.05$.

Since the QSH effect comes from the edge states due to the presence of a magnetic field, the stability of the spin Hall conductance $\sigma_{\rm s}^{\rm H}$ is related to the robustness of the edge states, which is determined by their density distributions. If the states are more localized near the edge, they have less chance to be scattered to the other edge with the opposite moving channel and thus are more robust to disorder. It shows in Fig. 7 that the disorder makes a sharp transition in the conductance curves becoming broader. The reason is that the transition energy one spin subsystem is near the plateau in the energy bands. Since the states there are more extended into the bulk, they are more likely to be destroyed by the disorder. This process can be shown more clearly by disordering the two-terminal conductance. Figure 8 shows the result of the calculations on the two-terminal device. Since the conductance is directly attributed to the edge states, the decrease in conductance means the breakdown of the edge states. As shown in Fig. 8, such breakdown happens near the plateau energy of a spin-up or spin-down subsystem.

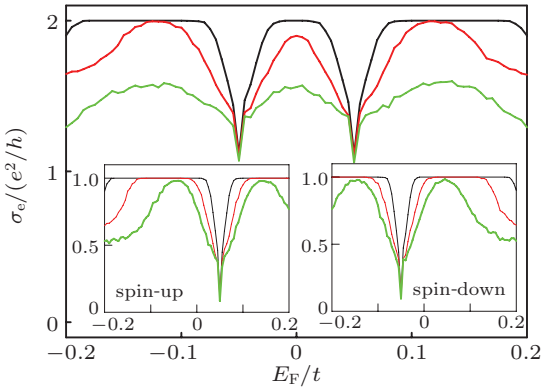


Fig. 8. (colour online) The robustness of the longitudinal conductance $\sigma_{\rm e}$ to a disorder for $M = 0.05$. The disorder strengths are $U_0/t = 1$ (black), $U_0/t = 2$ (red) and $U_0/t = 3$ (green). The two insets are for spin-up and spin-down subsystems respectively.

5. Conclusions

We have studied a square-lattice model under a uniform magnetic field. Using the Landauer–Büttiker formula, we have numerically calculated the longitudinal conductance on a two-terminal device, the Hall and spin Hall conductances on a four-terminal device, and the longitudinal and Hall resistances on a six-terminal device. These conductances and resistances are related to the edge states and exhibit quantized values. The quantized values are analytically derived and are in good agreement with those from numerical calculations.

In particular, for the cases with a ferromagnetic exchange split, the system exhibits a QSH effect. The resulting QSH effect is caused by the difference of the filling factors for spin-up and spin-down subsystems. It breaks TR symmetry and is in contrast to the Z_2 QSH insulator which is caused by TR preserving SOC. We also have studied the stability of the QSH effect to disorder and have found that the QSH effect is robust when the Fermi levels of both spin subsystems are far away from the energy plateaus but is fragile when the Fermi level of any spin subsystem is near the energy plateaus. These results provide an example of the QSH effect with a physical origin other than TR preserving SOC.

Acknowledgments

The authors are indebted to Jian Li, Qing-Feng Sun and Shun-Qing Shen for stimulating discussions.

References

[1] Moore J E 2010 *Nature* **464** 194
[2] Hasan M Z and Kane C L 2010 *Rev. Mod. Phys.* **82** 3045
[3] Qi X L and Zhang S C 2011 *Rev. Mod. Phys.* **83** 1057
[4] Qi X L and Zhang S C 2010 *Phys. Today* **63** 33
[5] Wang Z M 2011 *Acta Phys. Sin.* **60** 077203 (in chinese)
[6] Ma J,Luo H L and Wen S C 2011 *Acta Phys. Sin.* **60** 094205 (in Chinese)
[7] Tan Z B, Ma L, Liu G T, Lü L and Yang C L 2011 *Acta Phys. Sin.* **60** 107204 (in Chinese)
[8] Fu L and Kane C L 2008 *Phys. Rev. Lett.* **100** 096407
[9] Qi X L, Hughes T L and Zhang S C 2008 *Phys. Rev.* **78** 195424
[10] Essin A M, Moore J E and Vanderbilt D 2009 *Phys. Rev. Lett.* **102** 146805
[11] Seradjeh B, Moore J E and Franz M 2009 *Phys. Rev. Lett.* **103** 066402
[12] Kane C L andMele E J 2005 *Phys. Rev. Lett.* **95** 226801
[13] Bernevig B A,Hughes T L and Zhang S C 2006 *Science* **314** 1757
[14] Haldane F D M 1988 *Phys. Rev. Lett.* **61** 2015
[15] Kane C L and Mele E J 2005 *Phys. Rev. Lett.* **95** 146802
[16] Guo H M, Feng S P and Shen S Q 2011 *Phys. Rev.* **83** 045114
[17] Sun Q F and Xie X C 2010 *Phys. Rev. Lett.* **104** 066805
[18] Weeks C, Rosenberg G, Seradjeh B and Franz M 2007 *Nature Phys.* **3** 796
[19] Rosenberg G, Seradjeh B, Weeks C and Franz M 2009 *Phys. Rev.* **79** 205102
[20] Landauer R 1970 *Phil. Mag.* **21** 863
[21] Büttiker M, Imry Y, Landauer R and Pinhas S 1985 *Phys. Rev.* **31** 6207
[22] Datta S 1995 *Electronic Transport in Mesoscopic Symtems* (Cambridge: Cambridge University Press)
[23] Novoselov K S, Geim A K, Morozov S V, Jiang D, Zhang Y, Dubonos S V, Grigorieva I V and Firsov A A 2004 *Science* **306** 666
[24] Novoselov K S, Geim A K, Morozov S V, Jiang D, Katsnelson M I, Grigorieva I V, Dubonos S V and Firsov A A 2005 *Nature* **438** 197
[25] Novoselov K S, McCann E, Morozov S V, Fal'ko V I, Katsnelson M I, Zeitler U, Jiang D, Schedin F and Geim A K 2006 *Nature Phys.* **2** 177
[26] Zhang Y, Tan Y W, Stormer H L and Kim P 2005 *Nature* **438** 201